Quasi-Many-Body Localization in Translation-Invariant Systems

N. Y. Yao,[1] C. R. Laumann,[2,5] J. I. Cirac,[3] M. D. Lukin,[4] and J. E. Moore[1]
[1]Department of Physics, University of California, Berkeley, California 94720, USA
[2]Department of Physics, University of Washington, Seattle, Washington 98195, USA
[3]Max-Planck-Institut fur Quantenoptik, Hans-Kopfermann-Strasse 1, D-85748 Garching, Germany
[4]Department of Physics, Harvard University, Cambridge, Massachusetts 02138, USA
[5]Physics Department, Boston University, 590 Commonwealth Avenue, Boston, MA 02215, USA
(Received 7 November 2014; revised manuscript received 7 July 2016; published 7 December 2016)

We examine localization phenomena associated with generic, high entropy, states of a translation-invariant, one-dimensional spin ladder. At early times, we find slow growth of entanglement entropy consistent with the known phenomenology of many-body localization in disordered, interacting systems. At intermediate times, however, anomalous diffusion sets in, leading to full spin polarization decay on an exponentially activated time scale. We identify a single length scale which parametrically controls both the spin transport times and the apparent divergence of the susceptibility to spin glass ordering. Ultimately, at the latest times, the exponentially slow anomalous diffusion gives way to diffusive thermal behavior. We dub the intermediate dynamical behavior, which persists over many orders of magnitude in time, quasi-many-body localization.

DOI: 10.1103/PhysRevLett.117.240601

Understanding the interplay between interactions and disorder in quantum dynamics is among the central challenges in many-body physics. Since its proposal in 1958 [1], Anderson localization has been observed in disordered systems composed of photons, phonons, electrons, and ultracold atoms [2–4]. The physics of localization in each of these systems can be largely understood as a single-particle phenomenon. Extending disordered localization to the interacting many-body regime has attracted significant recent attention [5–38], in part, because it represents a fundamental breakdown of quantum statistical mechanics. This breakdown opens the door to a number of possibilities, including novel phase transitions in high-energy states, the protection of quantum and topological orders, and even the possibility of quantum information processing with disordered many-body systems [17,21,24,33,39,40].

A number of recent proposals have investigated the possibility that localization can persist even in the absence of disorder [34,35,41–45]. This idea can be traced back to early work on ^{3}He defects dissolved in solid ^{4}He [46,47]. There, it was proposed that a uniform system of strongly interacting narrow bandwidth particles could self-localize: A subset of the ^{3}He defects form immobile clusters which, in turn, block the diffusion of the remaining particles. In more recent proposals, the distinction between mobile and immobile particles is imposed manually. These models typically involve two types of particles, light and heavy; the dynamics of the heavy particles are significantly slower than those of the light particles [35,41]. At short time scales, interactions between the two flavors serve as a random quasistatic background potential for the light particles. If strong enough, this effective disorder can localize the light particles, and it has been argued that transport owing to the slow dynamics of the heavy particles is insufficient to delocalize the system. The central question which has emerged from these studies is whether randomness in the state of the system can be enough to cause "self-localization" and, what, precisely, does this mean?

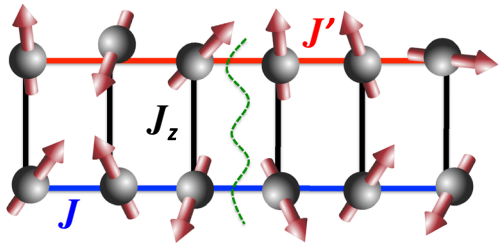

FIG. 1. Schematic of the one-dimensional spin-1/2 ladder. σ spins reside in the top chain and S spins in the bottom. Along each chain, the spins are coupled by nearest neighbor XY (flip-flop) interactions with strength J' and J, respectively. Across each rung, spins are coupled via Ising interactions of strength J_z. The green dotted line indicates the position of the cut used to divide the ladder when evaluating the entanglement entropy.

In this Letter, we address this question by considering a translation-invariant spin ladder (Fig. 1), whose two legs carry, respectively, the fast and slow particles. We find strong evidence for the existence of an exponentially diverging time scale $\tau \sim e^{L/\xi}$, which controls the decay of spin polarization at the longest available wave vector $k = 2\pi/L$. We term this quasi-many-body localization. This should be contrasted with the behavior observed in *disordered*, many-body localized spin chains where an initial polarization *fails* to decay even at infinite time.

For any finite wave vector k, we observe full polarization decay on a time scale consistent with $\tau(k) \sim e^{1/(k\xi)}$, *independent of system size*. Similar anomalous diffusion laws are seen in generalized Sinai models, where noninteracting particles diffuse in a random force field [48,49] and in the so-called spin trapping of one-dimensional ferromagnetic Bose gases [50]. The same exponential divergence with length scale ξ appears in the system's susceptibility to spin glass ordering [35]. In previous work, this has been taken to imply an instability toward spontaneous many-body localization. However, the presence of anomalous diffusion rules out this scenario. Moreover, at the latest times, we find that the exponentially slow anomalous diffusion ultimately gives way to diffusive thermal behavior.

Consider a two-leg, spin-1/2, ladder as shown in Fig. 1, with Hamiltonian

$$H = \sum_{\langle ij \rangle} J S_i^+ S_j^- + \sum_{\langle ij \rangle} J' \sigma_i^+ \sigma_j^- + \sum_i J_z S_i^z \sigma_i^z + \text{H.c.} \quad (1)$$

Spins of the lower (upper) chain are labeled S (σ) and are coupled via a nearest neighbor XY interaction of strength J (J'). The two spin species are coupled across a rung via Ising interactions of strength J_z [51]. In the limit $J' \to 0$, the σ spins of the upper chain can be viewed as classical variables that generate quenched disorder for their S-spin cousins. In this limit, fermionization of the S chain produces a noninteracting model which localizes for typical configurations of the $\{\sigma_i\}$. The introduction of a finite J' drives dynamics in the σ chain and effectively induces interactions in the system.

Entanglement dynamics.—We perform extensive exact diagonalization studies of Eq. (1). We consider periodic systems up to $N = 2L = 24$ sites and work at fixed filling $\nu_{s/\sigma} = 1/2$, where ν is the fraction of S/σ sites with spin up divided by L. All energies are normalized to $J = 1$. Our first diagnostic is the growth of entanglement entropy $S_{\text{ent}} = -\text{tr}\rho_A \log \rho_A$ across a central cut (parallel to a rung, Fig. 1) that divides the system in subregions A and B. Initial states are chosen to be random product states within the relevant Hilbert space, and we average over $\sim 10^2$–10^3 states depending on the system size. For short and intermediate time scales, much of the observed entanglement dynamics can be understood within the framework of spontaneous many-body localization (MBL) [35]. As we will see, it is only at the longest time scales that this framework fails and anomalous diffusion sets in.

We begin with strong effective disorder, $J_z = 10$, and measure the effect of a small $J' \ll J$. The result for $L = 4$, $J' = 10^{-3}$ is shown in Fig. 2(a) (see [52] for $J' = 10^{-2}$, 10^{-4}). We observe three plateaus in the growth of the entanglement entropy, which can be qualitatively understood as follows [Fig. 2(c)]. There is an initial growth of S_{ent} until time $t_1 \sim 1/J$, arising from the rapid expansion of wave packets to a size of the order of the noninteracting localization length. The first plateau is consistent with the entanglement behavior for single-particle-localized states and persists indefinitely for $J' = 0$.

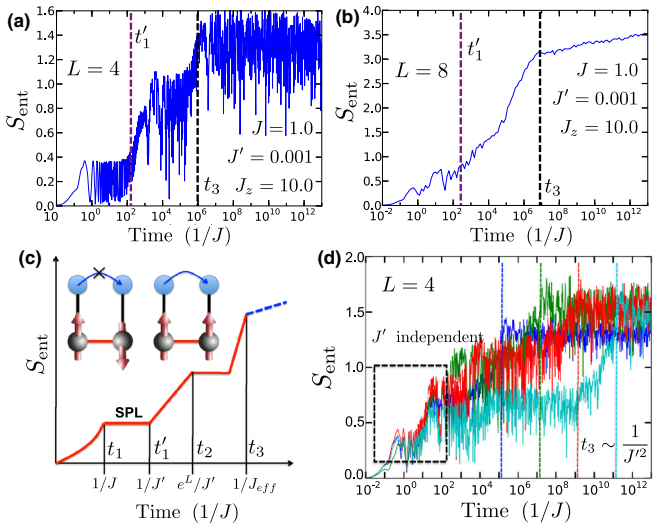

FIG. 2. (a) Growth of entanglement entropy for $L = 4$ sites, with $J' = 10^{-3}$ and $J_z = 10$. The entanglement entropy is averaged over 30 random initial product states. (b) Analogous data for $L = 8$ averaged over 100 random initial product states. (c) Schematic short-time entanglement entropy behavior. At $t_1 \sim 1/J$, a single-particle-localized (SPL) plateau is observed. At time scales $t_1' \sim 1/J'$, interactions set in and a logarithmic growth of entanglement begins. At $t_2 \sim e^L/J'$, this growth saturates for short chains unless it is preempted by the final "plateau" at $t_3 \sim 1/J_{\text{eff}} = (J'^2/J_z)^{-1}$ [52]. (d) $S_{\text{ent}}(t)$ for Heisenberg coupling along the ladders with $L = 4$, $J_z = 10$, and $J' = 10^{-2}$, 10^{-3}, 10^{-4}, 10^{-5}. Since there is no single-particle limit, the initial dynamics are J' independent, but t_3 continues to scale as $1/J'^2$.

At time scale $t_1' \sim 1/J'$ (purple dashed lines, Fig. 2), logarithmic growth of entanglement sets in [14,17], indicating that J' sets the time scale of interactions. The relevant dephasing process is shown in the inset in Fig. 2(c): The single-particle states of the S chain experience an energy shift dependent on their local occupation. This effective density-density interaction results from the hybridization of σ-chain orbitals on the time scale J'. Logarithmic growth progresses until the entanglement saturates at a second plateau, $t_2 \sim e^L/J'$. Up to now, the entanglement dynamics are consistent with those observed in disordered, MBL systems.

The second plateau corresponds to the complete, finite-size, dephasing of the S chain, while the dephasing dynamics of the slower σ chain have yet to begin. In principle, one might expect the third plateau to correspond to the finite-size entanglement saturation of the full system, with t_3 also scaling as $\sim e^L$. However, by numerically varying J', J_z, and L, we find instead that $t_3 \sim (J'^2/J_z)^{-1}$, with a weak, subexponential, L dependence [black dashed lines, Figs. 2(a) and 2(b)] [52]. At larger system sizes [Fig. 2(b)], the intermediate plateau disappears, since

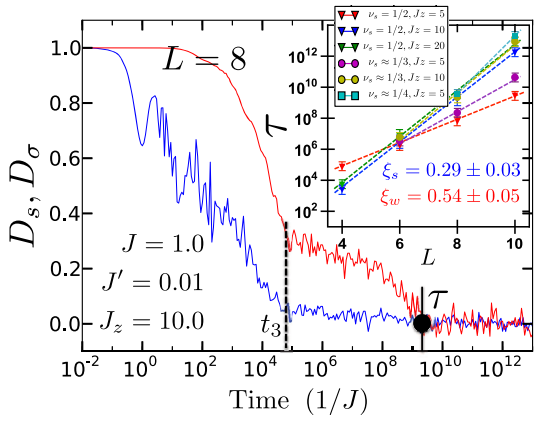

FIG. 3. A typical time trace of the decay of spin polarization. The blue line shows $D_s(t)$, while the red line shows $D_\sigma(t)$. The black dashed line indicates the position of t_3 as determined from the entanglement entropy, and the solid black line or dot depicts τ, the time at which all polarization has fully decayed. The inset depicts $\tau(k = 2\pi/L)$ as a function of the system size for $J_z = 5$, 10, 20 and filling fractions $\nu_s = 1/2, \nu_s \approx 1/3, 1/4$. For $\nu_s \approx 1/3$, $1/4$, commensuration effects at finite size prevent the choice of identical filling across sizes. For $\nu_s \approx 1/3$, the sizes are $L = 6$, 8, 10 with $\nu_s = 1/2, 3/8, 3/10$, respectively. For $\nu_s \approx 1/4$, the sizes are $N = 8$, 10 with $\nu_s = 1/4$, $1/5$, respectively [52]. The data at $\nu_s \approx 1/3$, $1/4$ are qualitatively consistent with saturation at strong effective disorder.

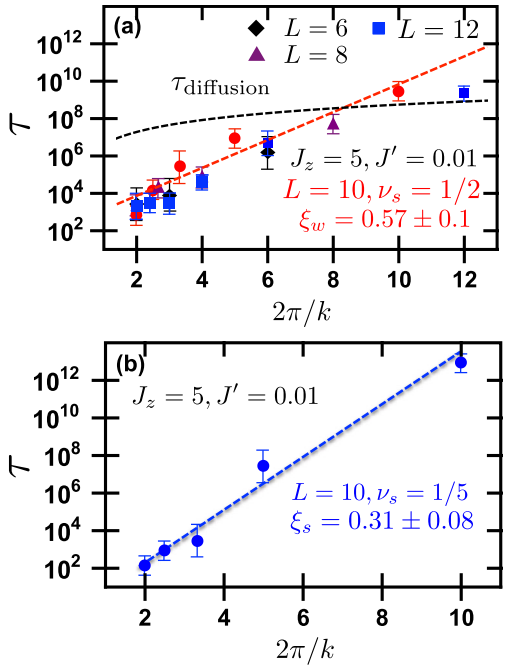

FIG. 4. τ as a function k. Data are obtained at $J_z = 5, J' = 0.01$. (a) Red circles correspond to $L = 10$ and filling $\nu_s = 1/2$, while (b) blue circles correspond to $L = 10, \nu_s = 1/5$. To confirm the L independence of the decay time, we also show data for $L = 6$, 8, 12 at a variety of k. The time scale for diffusive decay (as extrapolated from larger J' data) is shown as the black dashed line in (a); for small systems, $\tau_{\text{diffusion}}$ is so slow that the relaxation is limited by $e^{1/(k\xi)}$. However, for the largest system sizes, we observe the exponential quasi-MBL behavior to be cut off by an extremely slow diffusion.

$t_2 \sim e^L$ while t_3 does not; moreover, the third "plateau" begins to exhibit a clear upward drift, presaging additional dynamics to come.

This picture of entanglement growth is further confirmed by generalizing Eq. (1) to Heisenberg couplings within each chain. In particular, there is no longer a noninteracting regime, as is evidenced by the J' independent short-time dynamics in Fig. 2(d); meanwhile, the final plateau continues to depend quadratically on J' with weak L dependence. We return to intra-chain XY couplings for the remainder of the Letter.

Long-time dynamics.—To understand the long-time dynamics, it is helpful to turn to other physical quantities. In particular, we probe the decay of spin polarization as well as the susceptibility, χ to spin glass ordering [53]. As we will see, a *single* length scale, ξ, controls both as we vary J_z and ν_s (holding $\nu_\sigma = 1/2, J' = 0.01$). Indeed, the time scale τ for ultimate polarization decay scales as $\sim e^{L/\xi} = e^{2\pi/(k\xi)}$, while the susceptibility scales as $\sim e^{cL/\xi}$, for a constant c. In the $J' \to 0$ limit, J_z and ν_s directly control the effective disorder and thus the localization length ξ_0. From the observed behavior of $\xi(J_z, \nu_s)$, we surmise that it is continuously connected to ξ_0 as one turns off J'.

Polarization decay.—The decay of polarization D_s (D_σ) is a measure of spin transport at infinite temperature [11]. As each flavor of spin is separately conserved, we perturb the system with a small inhomogeneous spin modulation of the form $\hat{F}_s(k) = \sum_j S^z_j e^{ikj}$ (similarly for $\hat{F}_\sigma$) and measure the time-dependent relaxation of this polarization:

$$D_{s/\sigma}(k, t) = \langle e^{-iHt} F^\dagger_{s/\sigma}(k) e^{iHt} F_{s/\sigma}(k) \rangle, \qquad (2)$$

where the average is taken at infinite temperature.

A typical time series for $D_{s/\sigma}$ at the longest wavelength $k = 2\pi/L$ is depicted in Fig. 3. The most remarkable feature is the clarity of the various time scales. For example, the dashed line indicates the time scale t_3 as extracted from the corresponding entanglement entropy [52]. At this point, it is clear that there is still significant residual polarization. However, it is also clear that this polarization fully decays by time $\tau \sim 10^9/J$. The parametric dependence of $\tau(k = 2\pi/L)$ is illustrated in the inset in Fig. 3, where we plot its L dependence at fixed J_z and ν_s [45]; τ scales exponentially in system size which defines the length scale $\xi(J_z, \nu_s)$ as the inverse slope of the curves. For weak effective disorder $\nu_s = 1/2$, $J_z = 5$, we find $\xi_w = 0.54 \pm 0.05$. All other parameters correspond to stronger disorder, producing a shorter length, which saturates at $\xi_s = 0.29 \pm 0.03$ (extracted from $\nu_s = 1/2, J_z = 20$).

The existence of the length scale ξ suggests that finite wavelength inhomogeneities decay on a finite time scale $\tau(k) \sim e^{2\pi/(k\xi)}$. To test this hypothesis, we consider the ultimate decay time as a function of k for fixed L. For

$L = 10$, $J_z = 5$, and $\nu_s = 1/2, 1/5$ these data (circles) are plotted in Fig. 4 and are consistent with the proposed functional form (dashed line). This provides an independent means to extract ξ. We obtain $\xi_w = 0.57 \pm 0.1$ and $\xi_s = 0.31 \pm 0.08$ in agreement with the two lengths quoted above. To ensure that there is no system-size dependence lurking, we also plot $\tau(k)$ for $L = 6, 8, 12$. At the shared k value of $\pi/3$, $\pi/2$, $2\pi/3$, π, we find decay times which are identical (within error bars), further confirming the L-independent nature of the polarization decay. This demonstrates that all finite-k perturbations decay in a finite time.

The behavior $\tau(k) \sim e^{2\pi/(k\xi)}$ contrasts with many-body localization where inhomogeneities never decay. Given that polarization does decay, one expects diffusion to set in at long enough wavelengths. This is consistent with the observation of a crossover to diffusive decay, $\tau(k) \sim 1/k^2$ for $J' > 0.3$, wherein we extract a diffusion constant $D \approx 0.013 J'^2/J_z$ [52]. Extrapolating to $J' = 0.01$ yields the black dashed curve in Fig. 4(a), which cuts off the exponentially growing decay times for wavelengths $2\pi/k \gtrsim 9$. This is in strikingly good agreement with the three orders of magnitude suppression of τ at the largest numerically accessible wavelength $2\pi/k = 12$.

We dub the exponentially slow, pre-diffusive, dynamical regime: quasi-MBL.

Susceptibility.—Finally, we probe our system's susceptibility to spin glass ordering [35] by introducing a perturbation of the form

$$H_W = \sum_i h_i^z S_i^z + \sum_i h'^z_i \sigma_i^z, \tag{3}$$

where h and h' are independent random fields drawn from a uniform distribution of width W. To quantify the system's response to H_W, we consider an observable $\Delta\rho_\psi = \frac{1}{N}\sum_i^N |\langle\psi|S_{i+1}^z - S_i^z|\psi\rangle|$ which measures the inhomogeneity of the spin polarization in the S chain within an eigenstate ψ. We perform exact diagonalization on $H_T = H + H_W$ with $\nu_s = \nu_\sigma = 1/2$, $J' = 0.01$, $J_z = 5, 10, 20, 40$, and $10^{-6} < W < 10^{-4}$. We average over 10^3 disorder realizations for $N = 8, 12$ and over 10^2 realizations for $N = 16$; we also average $\Delta\rho$ over ten eigenstates centered around energy density $J/4$. Our results are depicted in Fig. 5. The inset indicates that $\rho(W)$ is in the linear response regime, as all data lie at slope one in the log-log plot.

It has been argued [35] that an exponential in system size divergence of $\chi = d\rho/dW$ reflects an instability toward many-body localization. We indeed observe such a dependence (Fig. 5). However, as previously discussed, we do not view the system as truly MBL, since spin transport occurs, albeit slowly, across the full system. In fact, the transport time appears to be precisely correlated with the divergence of the spin glass susceptibility. An analysis of the exponential dependence of $\chi \sim e^{L/\xi'}$ also yields an effective length scale (ξ') as a function of J_z (Fig. 5); for $J_z = 5$,

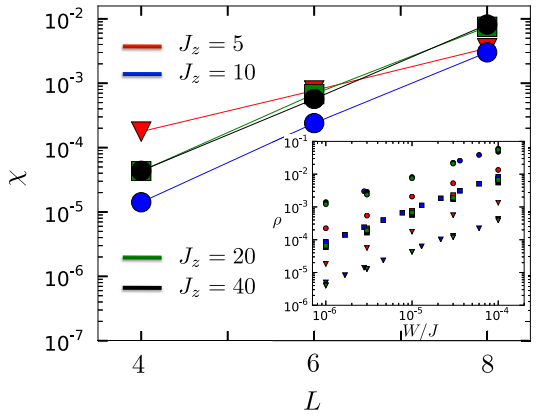

FIG. 5. (a) χ, the susceptibility to spin glass ordering as a function of system size L for $\nu = 1/2$ and $J_z = 5, 10, 20, 40$. The inset shows the raw $\rho(W)$ data used to generate the main figure. The value of χ is taken to be that of ρ at $W = 10^{-6}$. The slope of unity on the log-log plot demonstrates that we are clearly in the linear response regime.

$\xi' = 1.39 \pm 0.07$, and for $J_z = 10, 20, 40$, $\xi' = 0.77 \pm 0.08$. Interestingly, this length is in fact proportional to ξ, with a proportionality factor $c \approx 2.6 \pm 0.1$ across the data.

Discussion.—For a finite size system, translation invariance requires that, at an infinite time, any finite wavelength polarization must decay to zero. This follows immediately from Eq. (2) after inserting a resolution of the identity and dephasing off-diagonal matrix elements [55]:

$$D_{s/\sigma}(\infty) = \sum_\psi \langle\psi|F_{s/\sigma}^\dagger|\psi\rangle\langle\psi|F_{s/\sigma}|\psi\rangle. \tag{4}$$

As $F_{s/\sigma}$ carries nonzero momentum, its diagonal matrix elements vanish between translation-invariant many-body eigenstates $|\psi\rangle$. Thus, although disordered MBL systems exhibit finite residual polarization, we cannot expect that of any translation-invariant system. This algebraic truth does not rule out the possibility that the decay time $\tau(k)$ of finite wavelength polarization diverges with the system size. This is the natural definition of translation-invariant many-body localization.

While numerically accessible system sizes prohibit a complete characterization, we do not believe that such behavior holds. Rather, we find a finite decay time $\tau(k)$ for all k. All decay times, as well as the spin glass susceptibility χ, are controlled by a single physical length scale ξ. Crucially, this length scale is not simply related to the many-body density of states (inverse entropy). As previously discussed, we surmise that ξ is connected to the true localization length in the $J' \to 0$ limit [52], despite the fact that the system is not localized for any $J' \neq 0$. We have also numerically studied the behavior when the hoppings are closer in magnitude (but not equal, as then the model is integrable and different physics will apply); we find that relaxation onsets more rapidly at time

scales consistent with diffusive transport, $\tau_D \sim (L/a)^2 \hbar J/J'^2$ with no obvious sign of a phase transition.

In summary, we provide evidence that translation-invariant systems can exhibit quasi-MBL behavior intermediate between full localization and diffusion. This behavior is characterized by polarization decay on a time scale $\tau(k) \sim e^{1/(k\xi)}$, which in real space corresponds to an anomalous random walk with a mean square deviation growing as the log squared of time. Such anomalous diffusion is reminiscent of glasslike dynamics [34] and spin trapping in a one-dimensional ferromagnetic Bose gas [50], as well as generalized Sinai diffusion models [48,49]. It may also have qualitative similarities to the behavior observed in prethermalizing 1D multicomponent bosons [56,57] and in the glassy dynamics of asymmetric bosonic mixtures [58,59]. On the experimental front, quasi-many-body localization can be readily explored in a number of quantum optical systems, including trapped ions [60,61], polar molecules [62,63], and ultracold atoms [64].

It is a pleasure to gratefully acknowledge the insights of and discussions with Z. Papic, S. Gopalakrishnan, M. Knap, D. Huse, A. Chandran, S. Choi, S. L. Sondhi. This work was supported, in part, by DMR-1507141, the Simons Investigator program, the Miller Institute for Basic Research in Science, the NSF, the AFOSR-MURI, and the Sloan Foundation. C. R. L. acknowledges the hospitality of the Perimeter Institute and the Simons Institute for the Theory of Computing.

[1] P. W. Anderson, Phys. Rev. **109**, 1492 (1958).
[2] D. S. Wiersma, P. Bartolini, A. Lagendijk, and R. Righini, Nature (London) **390**, 671 (1997).
[3] T. Schwartz, G. Bartal, S. Fishman, and M. Segev, Nature (London) **446**, 52 (2007).
[4] S. S. Kondov, W. R. McGehee, J. J. Zirbel, and B. DeMarco, Science **334**, 66 (2011).
[5] L. Fleishman and P. W. Anderson, Phys. Rev. B **21**, 2366 (1980).
[6] B. L. Altshuler, Y. Gefen, A. Kamenev, and L. S. Levitov, Phys. Rev. Lett. **78**, 2803 (1997).
[7] D. Basko, I. Aleiner, and B. Altshuler, Ann. Phys. (Amsterdam) **321**, 1126 (2006).
[8] I. V. Gornyi, A. D. Mirlin, and D. G. Polyakov, Phys. Rev. Lett. **95**, 206603 (2005).
[9] A. L. Burin, arXiv:cond-mat/0611387.
[10] V. Oganesyan and D. A. Huse, Phys. Rev. B **75**, 155111 (2007).
[11] A. Pal and D. A. Huse, Phys. Rev. B **82**, 174411 (2010).
[12] M. Znidaric, T. Prosen, and P. Prelovsek, Phys. Rev. B **77**, 064426 (2008).
[13] C. Monthus and T. Garel, Phys. Rev. B **81**, 134202 (2010).
[14] J. H. Bardarson, F. Pollmann, and J. E. Moore, Phys. Rev. Lett. **109**, 017202 (2012).
[15] R. Vosk and E. Altman, Phys. Rev. Lett. **110**, 067204 (2013).
[16] S. Iyer, V. Oganesyan, G. Refael, and D. A. Huse, Phys. Rev. B **87**, 134202 (2013).
[17] M. Serbyn, Z. Papic, and D. A. Abanin, Phys. Rev. Lett. **110**, 260601 (2013).
[18] D. A. Huse and V. Oganesyan, Phys. Rev. B **90**, 174202 (2014).
[19] N. Y. Yao, C. R. Laumann, S. Gopalakrishnan, M. Knap, M. Müller, E. A. Demler, and M. D. Lukin, Phys. Rev. Lett. **113**, 243002 (2014).
[20] M. Serbyn, Z. Papic, and D. A. Abanin, Phys. Rev. Lett. **111**, 127201 (2013).
[21] D. A. Huse, R. Nandkishore, V. Oganesyan, A. Pal, and S. L. Sondhi, Nature (London) **502**, 76 (2013).
[22] D. Pekker, G. Refael, E. Altman, and E. Demler, Phys. Rev. X **4**, 011052 (2014).
[23] R. Vosk and E. Altman, Phys. Rev. Lett. **112**, 217204 (2014).
[24] Y. Bahri, R. Vosk, E. Altman, and A. Vishwanath, arXiv:1307.4092.
[25] B. Bauer and C. Nayak, J. Stat. Mech. (2013) P09005.
[26] M. Serbyn, M. Knap, S. Gopalakrishnan, Z. Papic, N. Y. Yao, C. R. Laumann, D. A. Abanin, M. D. Lukin, and E. A. Demler, Phys. Rev. Lett. **113**, 147204 (2014).
[27] R. Vasseur, S. A. Parameswaran, and J. E. Moore, Phys. Rev. B **91**, 140202 (2015).
[28] P. R. Zangara, A. D. Dente, P. R. Levstein, and H. M. Pastawski, Phys. Rev. A **86**, 012322 (2012); Phys. Rev. B **88**, 195106 (2013).
[29] S. Gopalakrishnan and R. Nandkishore, Phys. Rev. B **90**, 224203 (2014).
[30] R. Nandkishore, S. Gopalakrishnan, and D. A. Huse, Phys. Rev. B **90**, 064203 (2014).
[31] J. A. Kjall, J. H. Bardarson, and F. Pollmann, Phys. Rev. Lett. **113**, 107204 (2014).
[32] R. Nandkishore and A. C. Potter, Phys. Rev. B **90**, 195115 (2014).
[33] A. Chandran, V. Khemani, C. R. Laumann, and S. L. Sondhi, Phys. Rev. B **89**, 144201 (2014).
[34] G. Carleo, F. Becca, M. Schiro, and M. Fabrizio, Sci. Rep. **2**, 243 (2012).
[35] M. Schiulaz and M. Muller, AIP Conf. Proc. **1610**, 11 (2014).
[36] S. S. Kondov, W. R. McGehee, W. Xu, and B. DeMarco, Phys. Rev. Lett. **114**, 083002 (2015).
[37] M. Schreiber, S. S. Hodgman, P. Bordia, H. P. Lüschen, M. H. Fischer, R. Vosk, E. Altman, U. Schneider, I. Bloch, Science **349**, 842 (2015).
[38] J. Smith, A. Lee, P. Richerme, B. Neyenhuis, P. W. Hess, P. Hauke, M. Heyl, D. A. Huse, and C. Monroe, Nat. Phys. **12**, 907 (2016).
[39] N. Y. Yao, C. R. Laumann, and A. Vishwanath, arXiv:1508.06995.
[40] S. Choi, N. Y. Yao, S. Gopalakrishnan, M. D. Lukin, arXiv:1508.06992.
[41] T. Grover and M. P. A. Fisher, J. Stat. Mech. (2014) P10010.
[42] W. De Roeck and F. Huveneers, arXiv:1409.8054.
[43] J. M. Hickey, S. Genway, and J. P. Garrahan, J. Stat. Mech. (2016) 054047.
[44] Z. Nussinov, P. Johnson, M. J. Graf, and A. V. Balatsky, Phys. Rev. B **87**, 184202 (2013).

[45] M. Schiulaz, A. Silva, and M. Muller, Phys. Rev. B **91**, 184202 (2015).
[46] Y. Kagan and L. A. Maksimov, J. Phys. C **7**, 2791 (1974).
[47] Y. Kagan and L. A. Maksimov, Zh. Eksp. Teor. Fiz. **87**, 348 (1984).
[48] Y. G. Sinai, Theory Probab. Appl. **27**, 256 (1982).
[49] J.-P. Bouchaud and A. Georges, Phys. Rep. **195**, 127 (1990).
[50] M. B. Zvonarev, V. V. Cheianov, and T. Giamarchi, Phys. Rev. Lett. **99**, 240404 (2007).
[51] We note that the addition of a small flip-flop coupling across the rungs does not qualitatively change our results [52].
[52] See Supplemental Material at http://link.aps.org/supplemental/10.1103/PhysRevLett.117.240601 for methods and theoretical derivations.
[53] We ensure that our results are independent of the sampled energy density by comparing the extracted decay times from various energy density regions. Final result are averaged using states centered at energy densities $0.4J$, $J/3$, and $J/5$. Additionally, we verified that our results are not controlled by "mini-bands" [54].
[54] Z. Papic, E. M. Stoudenmire, and D. A. Abanin, Ann. Phys. **362**, 714 (2015).
[55] We assume that there are no additional lattice symmetries, such as reflection, which protect degeneracies.
[56] T. Kitagawa, A. Imambekov, J. Schmiedmayer, and E. Demler, New J. Phys. **13**, 073018 (2011).
[57] M. Gring, M. Kuhnert, T. Langen, T. Kitagawa, B. Rauer, M. Schreitl, I. Mazets, D. A. Smith, E. Demler, and J. Schmiedmayer, Science **337**, 1318 (2012).
[58] T. Roscilde and J. I. Cirac, Phys. Rev. Lett. **98**, 190402 (2007).
[59] T. Keilmann, I. Cirac, and T. Roscilde, Phys. Rev. Lett. **102**, 255304 (2009).
[60] A. Bermudez, J. Almeida, K. Ott, H. Kaufmann, S. Ulm, U. Poschinger, F. Schmidt-Kaler, A. Retzker, and M. B. Plenio, New J. Phys. **14**, 093042 (2012).
[61] J. Zhang, P. W. Hess, A. Kyprianidis, P. Becker, A. Lee, J. Smith, G. Pagano, I.-D. Potirniche, A. C. Potter, A. Vishwanath, N. Y. Yao, C. Monroe, arXiv:1609.08684.
[62] S. R. Manmana, E. M. Stoudenmire, K. R. A. Hazzard, A. M. Rey, and A. V. Gorshkov, Nature (London) **501**, 521 (2013).
[63] S. A. Moses, J. P. Covey, M. T. Miecnikowski, B. Yan, B. Gadway, J. Ye, and D. S. Jin, Science **350**, 659 (2015).
[64] R. Pires, J. Ulmanis, S. Häfner, M. Repp, A. Arias, E. D. Kuhnle, and M. Weidemüller, Phys. Rev. Lett. **112**, 250404 (2014).